Critical Criteria for Ignition of Combustible Fluids in Insulation Materials

J. Brindley
Dept. of Applied Mathematics, The University of Leeds, Leeds, LS2 95T, U.K.

J. F. Griffiths and J. Zhang
School of Chemistry, The University of Leeds, Leeds, LS2 95T, U.K.

N. A. Hafiz and A. C. McIntosh
Dept. of Fuel and Energy, The University of Leeds, Leeds, LS2 95T, U.K.

The possibility of a combustion hazard, when a flammable liquid leaks into insulation materials, is determined by the surface temperature, the volatility and loading of the fluid, the exothermicity of the combustion process, and the porosity of the matrix. Whether or not there is asymmetric heating is also influential. The oxygen diffusion rate or a reduction in its ambient concentration have a limited effect. A dimensionless, analytical, criticality criterion (u_∞) for ignition of flammable liquids dispersed within a hot inert matrix is compared with a dimensionless parameter (u_{FK}) based on the classic Frank–Kamenetskii ignition criterion. The relationship between u_∞ and u_{FK} is explored numerically over wide ranges of conditions and the switch as a monitor of safe operating practice are calculated assuming uniform surface heating. The application of u_∞ is most appropriate with a high loading of a relatively high volatility fluid dispersed within a matrix that presents a very high internal surface area, and the reaction is not very exothermic. The application of u_{FK} is appropriate to other circumstances. It was also found that certain classes of compounds may be capable of bonding to insulation in a way that suppresses their normal evaporative loss. This may signify a hitherto unrecognized problem that certain combinations of liquids and pipe insulating materials enhance combustion hazards.

Introduction

The practical motivation of this article is to establish criteria for the conditions at which spontaneous ignition may occur when a flammable liquid penetrates an insulation material surrounding a hot pipe, the so-called "lagging fire." This is a long-standing industrial problem that at least is a nuisance and, at worst, has been the cause of very considerable damage and commercial loss as a consequence of fire or explosion by it (Mellin, 1991; Gugan, 1974). Nevertheless, the problem has received relatively little attention, either through theory or through systematic experimental investigation (Gugan, 1974; Bowes, 1984; Britton, 1991).

If a fluid is dispersed over an extremely high internal surface area of the lagging, ignition may result from the exothermic oxidation of the fluid in contact with air within the hot, porous structure. Thus, although the basic mechanism for the combustion instability that leads to a lagging fire is similar to that for thermal ignition (Gray and Lee, 1968), additional considerations are the part played by mass transport of the flammable fluid both into and out of the insulation material across a boundary or within the inert matrix itself; vaporization of the fluid, which reduces the local concentration, and thereby affects the chemical reactivity; the "heat sink" effect owing to the enthalpy of vaporization and subsequent loss from the system; and a relationship to the porosity of the insulation. For most processes oxygen is essential for an exothermic reaction to occur, and its diffusion or limitation of access, as a result of displacement from the voids of the insulation as the liquid vaporizes, may also play a part.

Correspondence concerning this article should be addressed to J. F. Griffiths.

Currently, the practical assessment of the potential fire hazard within insulation relies on an empirical rule (Lindner and Seibring, 1967), an unsafe substance being determined from $AIT/(AIT - FP) > 1.55$, where AIT/°C and FP/°C are the autoignition temperature and flash point, respectively, of the combustible liquid. These temperatures are determined by specific tests as laid down by ASTM and CEC standards. Thus it is understood that ignition may be possible when a liquid can undergo exothermic oxidation (represented by AIT) at temperatures at which its volatility remains relatively low (represented by FP), but the relevance of loading of material, and the thermal conductivity, porosity, or thickness of the insulation are among the more serious omissions.

A mathematical model is developed here that indicates the physical situations that are at risk of spontaneous combustion, and from which practical criteria may be derived. The specific objectives addressed are the relevance of liquid volatility, the loading of a fixed amount of liquid, the matrix porosity, including oxygen diffusion and limitation, and the potential for scaling from laboratory studies to sizes and forms used in practical applications. Our research is based on a symmetrically heated block of insulation material, as adopted in experimental tests (Bowes and Langford, 1968; Bowes, 1984; Britton, 1991; McIntosh et al., 1994), and exemplified below. As in classic thermal ignition theory (Gray and Lee, 1968; Bowes, 1984), the simplest kinetic dependence of reaction is assumed, taking a first-order dependence on oxygen concentration in the gas phase and involving an interaction with the surface-dispersed liquid phase, the amount of which is governed by its local density within the insulation.

Aspects that are not considered at the present stage are the effect of asymmetric heating (as pertains to a lagged pipe), migration of the condensed fluid over the surface of the pore structure, a detailed consideration involving physical adsorption/desorption interactions, the consequence of a continuous supply resulting from a persistent leak at a joint in a pipe, any role of oxidation of the combustible material in the gas phase (McIntosh et al., 1997), or chain branching, kinetic mechanisms of the type normally associated with organic liquids and vapors at temperatures below 750 K (Griffiths, 1995).

The liquids involved are normally hydrocarbon based, such as the relatively high-volatility alkanes that compose the "low temperature heat transfer fluids" (for use up to 530 K) or mixtures of less volatile aromatic, and aliphatic hydrocarbons that make up the "high temperature heat transfer fluids" for use up to 670 K [such as *Santotherm* 59; boiling range 583–613 K, AIT = 683 K (410°C, FP = 411 K (138°C)]. These parameters yield the value 1.50 for the Lindner and Seibring criterion, indicating that it is a safe substance.

Diesel fuel may also present a hazard since its leakage in the engine rooms of ships and subsequent penetration into the lagging of hot pipes is a common occurrence. Other organic substances may also present a similar hazard. For example, ethylene glycol that leaked from a fractured joint in an insulation clad pipe was implicated as the cause of the destruction of a chemical plant in Antwerp in 1987 (Mellin, 1991). There is a diverse range of insulation materials, usually made up from glass fiber, mineral wool, or amorphous silicate compounds. They have different thermal insulation properties and densities, and may present significantly different surface/volume ratios within their structure. All of these factors may have important implications for fire or explosion risk.

Previous studies on the lagging fire problem

The experimental studies that have been reviewed by Bowes (1984) with respect to combustion of oil-soaked fibers, such as those of Taradoire (1926), relate mainly to conditions close to normal ambient temperatures, rather than the higher temperatures associated with hot pipes. Thus, although the amounts of fluid that impregnate the fiber may be relevant, the effect of evaporative loss on the response is not a primary consideration in such cases.

A theoretical and technical review of the lagging fire problem by Gugan (1974) reveals that a thermal ignition criterion derived for an asymmetrically heated hollow cylinder with internal heat transport by conduction (Thomas and Bowes, 1961; Bowes and Townshend, 1962) was deemed to be appropriate for the prediction of a critical temperature difference between inner and outer surfaces of a fluid-soaked lagging. This theoretical approach would be consistent with leakage of fluids that have a low volatility at the critical surface temperature, and may represent one extreme for the prediction of criticality in hot lagging.

Bowes and Langford (1968) performed a related experimental study to measure the minimum pipe temperature required for self-ignition when there was a controlled leak rate of a liquid into a fixed thickness of asymmetrically heated, insulation material. Complementary experimental studies were also made of the critical temperature for cubes of lagging that were uniformly heated in an oven and containing a fixed amount of the same liquid (Bowes and Langford, 1968). The insulation materials used were calcium silicate/asbestos and resin-bonded mineral wool, and the fluid was a low-viscosity transformer oil, which tended to have low volatility at the prevailing temperature ($T < 430$ K in the cube experiments). It was found that the critical temperature for uniformly heated cubes was lower than the critical temperature required at the hot surface of the asymmetrically heated pipe lagging (Bowes and Langford, 1968).

Critical temperatures of a range of compounds loaded to saturation in a variety of insulation material in the form of right cylinders (200 mm diam) were also measured by Lindner and Seibring (1967). These cylinders were then exposed to air that flowed over the cylinder surface at controlled rates while its temperature was raised at a rate of 10 K/h. Among the compounds that gave rise to spontaneous combustion were dimethyl terephthalate, triaryldimethane, cyclododecane, cyclododecanol, cyclododecanone, cyclohexane dimethanol, dimethyl hexahydroterephthalate, polystyrene, and lubricating oil.

The most extensive data on the performance of a number of classes of fluids dispersed within a variety of insulation materials were obtained in subsequent work by Britton (1991). Critical temperatures and induction times to self-heating or ignition were measured in experiments on 5-cm cubes of insulation, impregnated with controlled amounts of liquids, and held at constant temperature in an oven. Most of the fluids studied (amines, olamines, and glycols) were known to be reactive at fairly low temperatures and they had relatively high boiling points, so the competition between reactivity and volatility was not put to rigorous test.

Ignition delay times (t_{ign}) that exceeded 10 h were reported in a number of experiments by Britton (1991) and, for the glycols, these times extended to several days. Except at the margin of supercriticality, at which ignition delays are predicted to extend to infinite time (Gray et al., 1990), delays of this duration are incompatible with the thermal relaxation times for a 5-cm cube of any insulation material. Thus, even though these particular liquids were very involatile at the prevailing temperature ($T < 100$°C)—thus allowing the experiments to be considered approximate to those for classic thermal ignition studies—there is an underlying complexity of the behavior that cannot be interpreted on the basis of simple thermal ignition criteria.

In the present work, experiments were performed in which a high-temperature heat-transfer fluid (*Santotherm 59*; 40 cm^3) was soaked into 5-cm cubes, respectively, of an amorphous silicate (micropore) insulation and glass-fiber insulation packed into a wire-mesh basket. The respective matrix densities were 360 $kg \cdot m^{-3}$ and 240 $kg \cdot m^{-3}$. Each cube was fitted with a thermocouple located at the center (T1/T2, 0.1-mm-dia. wire) with a reference junction located external to the surface. Both cubes were located simultaneously in a preheated recirculating air oven set at 575 K, and the difference between the center temperature within each cube and the ambient (oven) temperature was recorded as a function of time using a potentiometric recorder.

As can be seen in Figure 1, in each case there is thermal runaway to achieve maximum center temperatures well in excess of 1,000 K, and the time to ignition was less than 1 h in the fiberglass system and about 3 h in the silicate insulation. These times included the initial heating time of each cube from laboratory temperature to that of the oven, which was approximately 30 min.

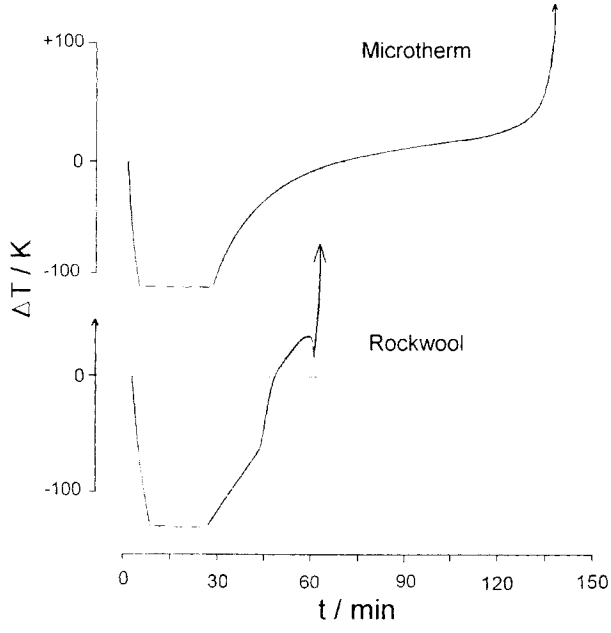

Figure 1. Experimental temperature–time records for the spontaneous ignition of a heat-transfer fluid within two different types of insulation material (5-cm cube) when exposed to a uniform surface temperature of 575 K within a preheated oven.

The temperature difference (ΔT) between the center and the surface of each cube was measured. The negative displacement represents the initial interval when the surface temperature exceeds that at the center.

It was shown also that the critical oven temperature below which thermal runaway did not occur was at 512 ± 2 K. There was no significant difference in the critical temperature between the two insulation materials despite their different densities, surface/volume ratios, and thermal conductivities. However, whereas the micropore material retained its integrity after thermal runaway, the fiberglass became a fused mass. This critical temperature for a lagging fire is appreciably below the quoted autoignition temperature of *Santotherm 59* (AIT = 683 K), and the occurrence of ignition would suggest that the empirical basis for assessing a potential lagging fire is hardly acceptable (Lindner and Seibring, 1967).

Theoretical Model

Against this background we have aimed to establish how the volatility of the fluid and its transport through the inert matrix affect the conditions for criticality, if the classic thermal ignition limit may be used as a reasonable basis for prediction of unsafe conditions, and in what circumstances the criticality criterion switches to fluid evaporation control. The numerical approach is underpinned by an analytical foundation on which the main conclusions are based (McIntosh et al., 1996). Generality is maintained by defining dimensionless groups to represent physical and chemical parameters, which are explained below. However, for the numerical results reported here, it has been necessary to adopt quantitative values for the physical properties of the insulation material and the physicochemical properties of the reactive fluid. Some of these are well defined, but others have to be estimated. A high-performance, microporous thermal insulation is considered for the present purpose, formed as a rigid moulded shape comprising bonded ceramic powders with reinforcing ceramic fibers. The relevant properties are given in Table 1.

The microporous insulation has an open cellular structure with average cell dimension of less than 0.1 μm. This dimension is so sufficiently small that gaseous molecule motion may fall in the Knudsen flow regime. While this does not affect the form of the representation of gaseous diffusion in the numerical model, it does mean that, in reality, species diffu-

Table 1. Characteristics of Microporous Thermal Insulation

Physical form	Rigid and flexible sheets or moulded shapes
Composition	Bonded ceramic powders with reinforcing ceramic fibers
Structure	An open cellular structure
Cell dimension	< 0.1 μm (av.)
Porosity (γ)	90% voidage (approx.)
Thermal conductivity (λ)	0.025 ± 0.05 $W \cdot m^{-1} \cdot K^{-1}$ over the range 0–400°C
Density (ρ)	200–400 $kg \cdot m^{-3}$
Heat capacity (c)	800–1,000 $J \cdot kg^{-1} \cdot K^{-1}$ over the range 0–400°C

sion may be governed by relative molecular mass and may not be affected by the overall composition of the gas mixture in the voids.

Model and assumptions

The geometries that may be represented by a single characteristic dimension are the infinite cylinder, the infinite slab, and the sphere, and the following analytical treatment refers to these cases. The following assumptions are made:

1. Reactant is adsorbed in the liquid state on the pore surface within the insulation matrix. It may react in this condensed state or it may evaporate, the vapor being assumed to be inert. There is no inhomogeneity of the surface sites.
2. Exothermic oxidation occurs by reaction between gaseous oxygen in the pores and the condensed reactant, this being interpreted as a single-step reaction that is first order with respect to the gas-phase oxygen concentration and the condensed fluid density.
3. Vaporization is related to the condensed fluid density, and its temperature dependence is controlled by the enthalpy of vaporization.
4. Exponential temperature dependences are assumed for the reaction- and evaporation-rate coefficients.
5. Conductive heat transfer and oxygen diffusion are assumed to occur in accordance with Fourier's and Fick's laws, respectively. Convective heat transport of gaseous components is ignored, as are pressure gradients within the matrix.
6. There is no resistance to heat transport at the surface ($Bi = \infty$).

The set of appropriate time-dependent, partial differential equations represent a special application of the diffusion-reaction equations, which are analyzed in a formal way by Aris (1975). The model variables are the matrix temperature, $T(r,t)$, the molar density of condensed reactant, $X(r,t)$, and the concentrations of fuel vapor, $Y(r,t)$ and oxygen $Z(r,t)$, each expressed as a function of spatial coordinate r and time t. The respective conservation equations are expressed in the form:

$$\rho c \frac{\partial T}{\partial t} = \underbrace{QAXZ \exp^{(-E/RT)}}_{\text{chemical heat release rate}} - \underbrace{Q_V FX \exp^{(-E_V/RT)}}_{\text{endothermic vaporization rate}} + \underbrace{\lambda\left(\frac{\partial^2 T}{\partial r^2} + \frac{j\partial T}{r\partial r}\right)}_{\text{thermal conduction rate}} \quad (1)$$

$$\frac{\partial X}{\partial t} = \underbrace{-AXZ \exp^{(-E/RT)}}_{\text{chemical consumption rate}} - \underbrace{FX \exp^{(-E_V/RT)}}_{\text{evaporative loss rate}} + \underbrace{D_F\left(\frac{\partial^2 X}{\partial r^2} + \frac{j\partial X}{r\partial r}\right)}_{\text{mass diffusion rate}} \quad (2)$$

$$\frac{\partial Y}{\partial t} = \underbrace{FX \exp^{(-E_V/RT)}}_{\text{evaporative generation rate}} + \underbrace{D_V\left(\frac{\partial^2 Y}{\partial r^2} + \frac{j\partial Y}{r\partial r}\right)}_{\text{mass diffusion rate}} \quad (3)$$

$$\frac{\partial Z}{\partial t} = \underbrace{-AXZ\nu \exp^{(-E/RT)}}_{\text{chemical consumption rate}} + \underbrace{D_0\left(\frac{\partial^2 Z}{\partial r^2} + \frac{j\partial Z}{r\partial r}\right)}_{\text{mass diffusion rate}}. \quad (4)$$

The term on the lefthand side of the energy conservation equation (Eq. 1) represents the volumetric heat capacity (ρc). In principle, this should be summed over all species within the matrix, and this could change considerably if there are very substantial loadings of fluid initially. It is assumed that the fuel loading is sufficiently small that a constant value for ρc, representing the inert matrix, is satisfactory. The shape factor j in the thermal and mass diffusion terms takes the values 0, 1, and 2, respectively, for the infinite slab (thickness $2l$), infinite cylinder (radius l), and sphere (radius l). The chemical consumption rate in Eq. 4 includes a stoichiometric coefficient ν for the relative number of moles of oxygen consumed per mole of fuel reacted. All terms defined in the text appear in the Notation section.

Nondimensionalization of equations and reduced parameters

To facilitate analytical interpretation, and to generalize the predicted behavior it is appropriate to nondimensionalize Eqs. 1–4. We have adhered to the groups normally associated with thermal ignition theory. The characteristic time is based on the Fourier time t_F ($= l^2\rho c/\lambda$, where l is the radius or half thickness). Temperature is nondimensionalized with respect to the temperature coefficient for the chemical reaction (E/R), and given as u (Gray and Wake, 1988). The reason for this particular choice is that, by contrast to the more common Frank-Kamenetskii parameter $\theta = E\Delta T/RT_a^2$ (Gray and Lee, 1968; Frank-Kamenetskii, 1969), or $\nu = T/T_a$ (Aris, 1975), the ambient temperature is not included in u. This means that T_a (or u_a) can be used as an independent control parameter to explore the properties of the system. The species are nondimensionalized with respect to the initial molar densities of the uniformly distributed fluid (X_O) and the initial oxygen (Z_O) within the insulation block, which is taken to be the same as the external oxygen concentration. Thus we write

$$\tau = \frac{t}{t_F}, \quad u = \frac{RT}{E}, \quad x = \frac{X}{X_O}, \quad y = \frac{Y}{X_O},$$

$$z = \frac{Z}{Z_O}, \quad \text{and} \quad \beta = \frac{E_V}{E}.$$

Reduced parameters are also used as follows.

$$q = \frac{QX_O R}{\rho c E}, \quad q_V = \frac{Q_V X_O R}{\rho c E}, \quad a_1 = AZ_O t_F,$$

$$a_2 = \frac{\nu X_O a_1}{Z_O}, \quad f = Ft_F.$$

The dimensionless exothermicity q is equal to the dimensionless adiabatic temperature excess following complete consumption of the reactant in the absence of any vaporization. Similarly, q_v is equal to the dimensionless temperature decrease owing to complete vaporization of the reactant with no reaction. The Lewis numbers, which represent the ratio of mass diffusivity to thermal diffusivity are given by

$$L_F = \frac{D_F \rho c}{\lambda}, \quad L_V = \frac{D_V \rho c}{\lambda}, \quad L_O = \frac{D_O \rho c}{\lambda}.$$

L_F relates to surface migration of the fluid (D_F), and so is taken to be zero in the present application. Equations 1–4 can then be represented in the nondimensionalized and reduced form:

$$\frac{\partial u}{\partial \tau} = qa_1 xz \exp^{(-1/u)} - q_v fx \exp^{(-\beta/u)} + \left(\frac{\partial^2 u}{\partial \xi^2} + \frac{j \partial u}{\xi \partial \xi} \right) \quad (5)$$

$$\frac{\partial x}{\partial \tau} = -a_1 xz \exp^{(-1/u)} - fx \exp^{(-\beta/u)} + L_F \left(\frac{\partial^2 x}{\partial \xi^2} + \frac{j \partial x}{\xi \partial \xi} \right) \quad (6)$$

$$\frac{\partial y}{\partial \tau} = fx \exp^{(-\beta/u)} + L_V \left(\frac{\partial^2 y}{\partial \xi^2} + \frac{j \partial y}{\xi \partial \xi} \right) \quad (7)$$

$$\frac{\partial z}{\partial \tau} = -a_2 xz \nu \exp^{(-1/u)} + L_O \left(\frac{\partial^2 z}{\partial \xi^2} + \frac{j \partial z}{\xi \partial \xi} \right). \quad (8)$$

Stationary-state solutions and limiting conditions

As set out in the Introduction, there are two limiting physical conditions for a lagging fire to develop. The first is that of a fluid that is sufficiently involatile at the critical temperature that its behavior resembles thermal ignition under Frank-Kamenetskii conditions (Frank-Kamenetskii, 1969). Most examples of lagging fires that have been studied so far appear to approach this extreme (Bowes and Langford, 1968; Britton, 1991). This condition may be represented as a stationary state solution to Eq. 6 in the limit of no evaporation (McIntosh et al., 1996). Thus, Eq. 5 takes the form

$$\frac{\partial u}{\partial \tau} = qa_1 xz \exp^{(-1/u)} + \left(\frac{\partial^2 u}{\partial \xi^2} + \frac{j \partial u}{\xi \partial \xi} \right). \quad (9)$$

Invoking the Frank-Kamanetskii exponential approximation and assuming constant x and z, Eq. 9 can be solved to give the classic solution:

$$\delta_{cr} = \frac{qa_1 xz}{u_{FK}^2} \exp^{(-1/u_{FK})} = \frac{QAEX_O Z_O l^2}{\lambda R T_{FK}^2} \exp^{(-E/RT_{FK})}, \quad (10)$$

where the Frank-Kamanetskii parameter, δ_{cr}, takes the values 0.878, 2.00, and 3.32, respectively, for the shape parameters $j = 0$, 1, and 2. Equation 10 can be solved numerically for a given shape (Boddington et al., 1971) to give the *critical* dimensionless ambient temperature u_{FK} or, in dimensional form, T_{FK}.

The second limiting condition arises when the volatility of the fluid is sufficiently high that the propensity for thermal runaway is controlled entirely by an interaction between the chemical heat release rate and the endothermic evaporation rate (McIntosh et al., 1996). This condition can also be interpreted from a stationary state solution of Eq. 6 involving only the first and second terms on the righthand side. Thus, If x and z are assumed constant, a dimensionless critical temperature (u_∞) can be derived, in the analytical form

$$u_\infty = \frac{(1-\beta)}{\ln(qa_1 z) - \ln(q_v f)}. \quad (11)$$

For $u < u_\infty$, the system is not endothermic and is not subject to any temperature rise. This represents one extreme for an inherently safe system, and is a more fundamentally based representation of the properties encapsulated in the empirical equation introduced by Lindner and Seibring (1967).

From comparisons of numerical solutions to Eqs. 5–8, we show later that the two criteria u_{FK} and u_∞, derived from Eqs. 10 and 11, may be regarded as representative of lower bounds for a safe maximum operating temperature with respect to circumstances in which reactant consumption or loss occurs (which is represented by a parameter u_a^*, and is defined below). We establish also the conditions where the switch from u_∞ to u_{FK} would become appropriate as a criterion for safe operation.

Input Parameters and Numerical Methods

In order to derive numerical solutions, it is essential to deduce suitable values for the parameters involved. However, in the nature of the chemical and physical simplifications that have had to be made to retain the analytical tractability shown in Eqs. 10 and 11, approximations and estimates have to be made for some of the parameters. The fully dimensionalized input parameters are given in Table 2, and are explained as follows.

Thermochemical and kinetic parameters

If the fluids that are most likely to be encountered in lagging fires are hydrocarbon based, then the $-CH_2-$ moiety may be regarded as a representative part of the chemical structure. Its complete oxidation is given by

$$-CH_2- + 3/2\,O_2 = CO_2 + H_2O, \quad (12)$$

from which the overall heat of combustion (Q) is 4.4×10^7 $J \cdot kg^{-1}$ of the reactant. However, most of this energy is released in the late stages of reaction since many competitive and consecutive free-radical chain -propagation and branching processes are involved, which lead to complex mixtures of partially oxidized or degraded intermediates prior to the formulation of the final products (Griffiths, 1996). The onset of spontaneous ignition of hydrocarbons is known to evolve at low temperatures ($T < 700$ K) through organic peroxides and other partially oxygenated intermediates, and it is the exothermicity associated with the reactions appropriate to this temperature range that should be used to represent Q in determining the critical criteria for spontaneous ignition. While it is not possible to represent this low-temperature hydrocar-

Table 2. Physical and Chemical Parameters

Exothermicity $Q/J \cdot kg^{-1}$	2.34×10^6
Enthalpy of vaporization $Q_V/J \cdot kg^{-1}$	3.80×10^5
Preexponential factor (reaction) $A/kg^{-1} \cdot m^3 \cdot s^{-1}$	1.5×10^{13}
Preexponential factor (vaporization) F/s^{-1}	5.8×10^3
Activation energy (reaction) $E/J \cdot mol^{-1}$	1.5×10^5
Activation energy (vaporization) $E_V/J \cdot mol^{-1}$	6.5×10^4
Liquid diffusion coeff. $D_F/m^2 \cdot s^{-1}$	0
Vapor diffusion coeff. $D_V/m^2 \cdot s^{-1}$	1.0×10^{-5}
Oxygen diffusion coeff. $D_O/m^2 \cdot s^{-1}$	1.0×10^{-5}
Stoichiometry coeff. ν	0.3

bon oxidation chemistry by reference to the $-CH_2-$ moiety in isolation, its partial oxidation might be thought to take either of the forms

$$-CH_2-+1/2\ O_2=CO+H_2 \qquad (13)$$

or

$$-CH_2-+1/2\ O_2=CH_2O. \qquad (14)$$

In each of these cases the enthalpy of reaction is approximately -6.5×10^6 J·kg^{-1}, which testifies to the relatively small proportion of the overall heat release that is associated with the onset of combustion. In order to allow for the still lower exothermicity associated with peroxide formation, in the present calculations Q is taken to be 2.5×10^6 J·kg^{-1}.

The activation energy associated with peroxide-forming processes may be expected to be in the range 150 to 200 kJ mol^{-1} (Snee and Griffiths, 1989). The representation of the chemistry as a single-step, first-order reaction requires the preexponential factor (A) to be obtained empirically. This parameter was obtained by matching u_a^* to the critical temperature obtained for $n-C_{10}H_{21}OH$ (Table 3). This compound was one of the series of high molar mass alcohols that were investigated by McIntosh et al. (1994).

Vaporization characteristics

The fluid vaporization rate has been represented in exponential form, related to the Clausius–Clapeyron equation for the temperature dependence of the vapor pressure of liquids. This means that the enthalpy of vaporization determines not only the endothermicity of the vaporization process but also the temperature coefficient for the rate at which the vapor is generated. The temperature coefficient is expressed as an activation energy for the vaporization process (E_V) in Table 2. The enthalpy of vaporization falls in the range 50–75 kJ·mol^{-1} for liquids with boiling points up to about 650 K, the higher values being associated with more polar or high-boiling-point liquids. This yields a typical enthalpy of vaporization $Q_V=3.8\times10^5$ j·kg^{-1} for fluids of relative molar mass in the range 130 to 200. It is extremely difficult to assess the vaporization rate coefficient F, and so this was derived from comparisons with the combustion measurements made by McIntosh et al. (1994).

It is assumed that a known amount of fluid is soaked uniformly within the block of insulation initially and that there was air present throughout the porous structure. The initial temperature is set at the control temperature of the oven (T_a) and is uniform through the block. Hence the dimensionless initial conditions are $u(\xi,0)=u_a$, $x(\xi,0)=1$, $y(\xi,0)=0$, and $z(\xi,0)=1$.

The system of parabolic differential equations was solved numerically using the NAG library routine D03PBF, taking forty uniformly distributed nodes in the spatial coordinate in order to obtain reasonably accurate results. The integration step size was controlled by a tolerance parameter for the estimation of the local error, which was varied in the range 10^{-6} to 10^{-10}.

Table 3. Experimentally Measured Critical Temperatures for Normal Alcohols in a 5-cm Cube of Microtherm

Alcohol	B Pt/K	T_{cr}/K	u_a^* (±0.0001)
n-$C_{11}H_{23}OH$	515.5	429 ± 2	0.02378
n-$C_{10}H_{21}OH$	504	433 ± 1	0.02400
n-$C_9H_{19}OH$	488	433 ± 1	0.02400
n-$C_8H_{17}OH$	468	444 ± 2	0.02461
n-$C_7H_{15}OH$	444	444 ± 2	0.02461

From: McIntosh et al. (1994).

Numerical Results

Recognizing ignition

To first determine the minimum ambient temperature at which thermal runaway occurs, the temporal evolution at the center of the insulation block ($0.5<\xi<1$) is traced over a range of values of u_a, all other parameters being fixed. The minimum ignition temperature (u_a) falls within a region of parametric sensitivity of the transient dimensionless temperature maximum as reaction proceeds (Figure 2, upper). In these examples a difference of 1% is taken between the magnitude of u_a for the highest subcritical and lowest supercritical reactions, which is about the precision of most experimental measurements. The mean value is interpreted as the *watershed temperature*, u_a^*.

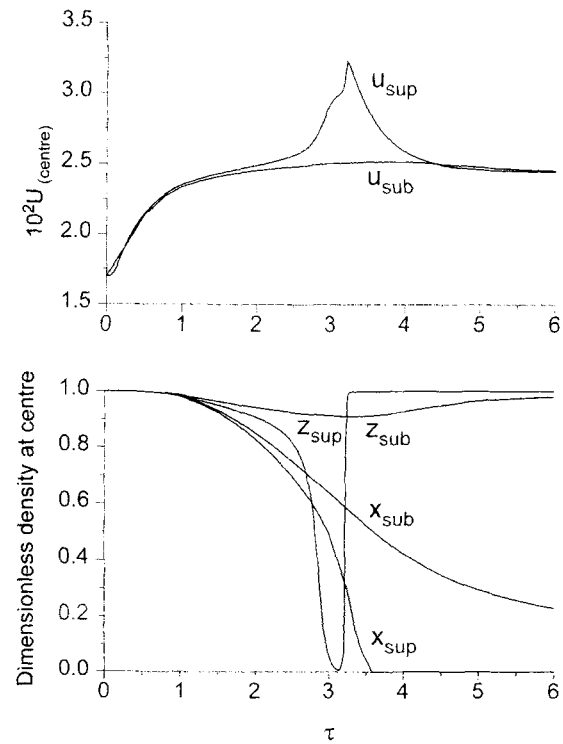

Figure 2. Numerical simulations of the parametric sensitivity at criticality when a liquid dispersed in insulation material is exposed to initial temperatures that differ by 1%.

The upper record shows the temporal evolution of the dimensionless center temperature (U_{center}). The lower records show the corresponding changes in dimensionless condensed fuel density (x) and the dimensionless oxygen density (z), all as a function of the Fourier time (τ).

The corresponding profiles for the dimensionless oxygen concentration and the condensed fluid density at the center of the block are shown in Figure 2 (lower). Whereas very little oxygen is consumed during the course of subcritical reaction, there is complete consumption at the center of the block in supercritical conditions, and this depletion of oxygen proves to be the reaction-rate limiting factor. The subsequent recovery of the oxygen concentration occurs because residual fuel is forced to evaporate as the temperature increases during combustion, and so no further reaction is possible. The distinction between the subcritical and supercritical fuel density profiles is less marked than that for the oxygen concentration because there is a significant contribution to the reduction of the fuel density by the evaporative process regardless of whether or not much oxidation occurs.

Effect of volatility

The vaporization of the fuel is characterized in nondimensional terms in Eqs. 5–8 by the dimensionless fuel vaporization coefficient, f, and its enthalpy of vaporization, q_v. The numerical solution for u_a^* and the dependences of u_∞ and u_{FK} on f are given in Figure 3. Whereas the Frank-Kamenetskii criterion, u_{FK}, is independent of f, u_∞ increases monotonically from $u_\infty = 0$ at $f = 0$ to $u_\infty = \infty$ at $f = qa_1 z/q_v$ (Eq. 11), where $\log f = 17.37$ from the present data. There is a crossing point of the curves that represent u_∞ and u_{FK}. The numerically computed watershed temperature, u_a^*, is asymptotic to u_{FK} at low f, but shows a highly nonlinear departure in the vicinity of the crossing point between u_{FK} and u_∞. However, at higher values of f, u_a^* does not follow u_∞, but reaches its own asymptote. The reasons for this are connected with the enhancement of the rate of fluid loss by vaporization from the system, which causes sufficient depletion of the remaining liquid (given by the dimensionless parameter x) that the rate of heat release by oxidation rate is itself curtailed. The departure from u_∞ arises because the analytical solution for u_∞ is derived for a value of x that is assumed to be constant.

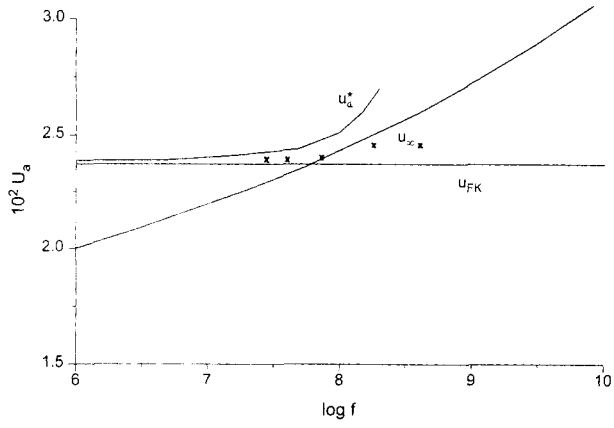

Figure 3. Dependence of u_a^*, u_∞, and u_{FK} on the dimensionless vaporization coefficient (log f).

A typical value for log f is 7.6, such as is required to represent the experimental results obtained by McIntosh et al. (1994). This is close to the transition between the u_∞ and u_{FK} criticality criteria. The experimental points are derived from data given in Table 4.

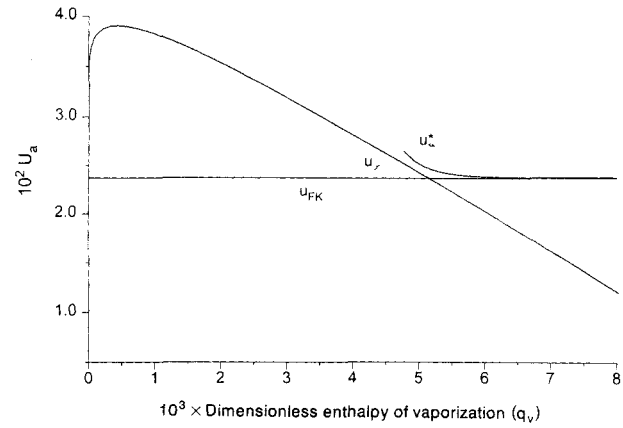

Figure 4. Dependence of u_a^*, u_∞, and u_{FK} on the dimensionless enthalpy of vaporization (q_v).

A typical value for q_v is 6.25×10^{-3}.

Also marked on Figure 3 are representations of the critical conditions obtained from the experimental results given in Table 3. The purpose of this comparison is to demonstrate a transition from the applicability of the Frank-Kamenetskii criterion (u_{FK}) to one that is determined by the evaporation process (u_∞). Values of u_a^* for each compound were derived directly from T_{cr}. They span the range from 0.0238 for $n-C_{11}H_{23}OH$, which is the alcohol of lowest volatility, to 0.0246 for $n-C_7H_{15}OH$. The values for f were calculated from that for $n-C_{10}H_{21}OH$, based on the relative magnitudes of the vapor pressures of each alcohol at its respective critical temperature.

The dependence of u_a^*, u_∞, and u_{FK} on q_v are shown in Figure 4. There is no dependence of u_{FK} on q_v and, at high q_v, the numerically determined value of u_a^* becomes asymptotic to it. The dependence of u_∞ on q_v is controlled not only by the explicit term $\ln q_v$ but also implicitly through variation of β, which appears in Eq. 11. The dependence of β on q_v arises from the temperature dependence of the vaporization rate, which is represented by the enthalpy of vaporization in the Clausius–Clapeyron equation.

Throughout most of the range of q_v, u_∞ falls almost linearly from its maximum at low q_v. This predicted fall is governed predominantly by the decreasing rate of vaporization as β increases. However, in the limit $q_v \to 0$ there is a negligible effect of the change of β, whereas $\ln q_v$ is quite strongly affected. The increase of q_v determines the sharp increase in u_∞ from zero to its maximum. The watershed temperature begins its departure from u_{FK} in the vicinity of the crossing point between u_∞ and u_{FK} (at $q_v = 0.052$) and, for similar reasons to those connected with Figure 3, u_a^* reaches an asymptotic limit with respect to q_v.

Effect of liquid fuel loading

The computer watershed temperatures, u_a^*, are shown in Figure 5 as a function of the initial loading of the fuel. The predicted values of u_a^* become asymptotic to u_∞ at very high loadings, but there is a significant departure from u_∞ as the loading falls, so as to cause u_a^* eventually to follow the u_{FK} curve reasonably closely. The experimental results that were reported in our earlier work (McIntosh et al., 1994) corre-

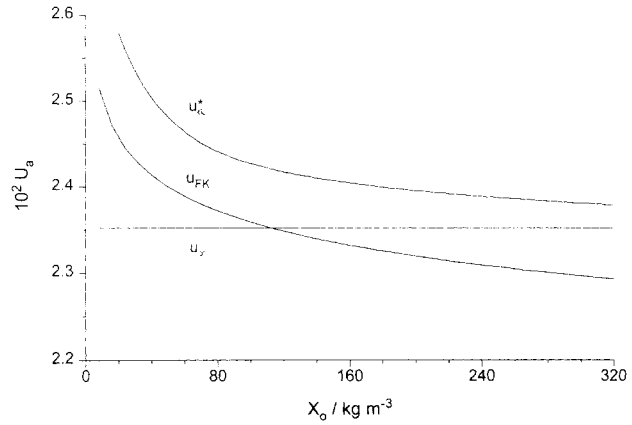

Figure 5. Dependence of u_a^*, u_∞, and u_{FK} on the initial loading of fuel in the insulation (X_O).

A loading of 80 kg·m^{-3} was adopted in the experiments reported by McIntosh et al. (1994). Loadings of over 300 kg·m^{-3} have been used in other experiments (Britton, 1991).

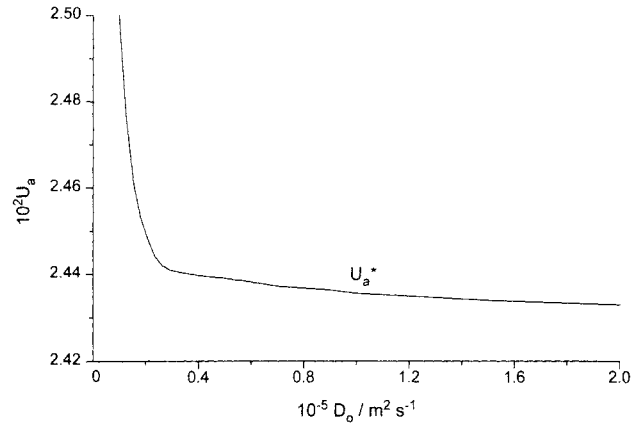

Figure 6. Dependence of u_a^* on the diffusion coefficient for oxygen (D_O).

The highest value shown ($D_O = 2.0\times10^{-5}$ m^2·s^{-1}) would represent normal diffusion. The porosity of the insulation matrix would reduce the effective diffusion coefficient. Both u_∞ and u_{FK} ($< u_a^*$) are independent of D_O.

spond to rather light loadings of 80 kg·m^{-3}, whereas those of Britton (1991) were rather heavier, generally exceeding 200 kg·m^{-3}.

Role of oxygen diffusion and of the external concentration of oxygen

The highest permissible diffusion coefficient for oxygen may be reasonably assumed to be about 1.8×10^{-5} m^2·s^{-1}, which is its diffusion coefficient at normal conditions. A lower value would relate empirically to an effect of the porosity of the insulation material. Bowes and Thomas (1966) suggested a correction factor of 0.6 to the value of D_O in air for diffusion in packed, hardwood sawdust, and the reduction could be much greater in materials of lower porosity. Nevertheless, the practical value of the Lewis number (L_O) would exceed 50, and could approach 200 at the upper limit for the diffusion coefficient of oxygen. This is considerably higher than that associated with flames burning in air, for which the Lewis number is normally close to unity.

As shown in Figure 6, the predicted values for u_a^* are highly sensitive to D_O over the range $0–0.3\times10^{-5}$ m^{-2}·s^{-1}, but there is hardly any further variation in u_a^* throughout the rest of the range. The watershed condition u_a^* always lies above u_{FK} and u_∞, where $u_{FK} = 0.0237$ and $u_\infty = 0.0235$ in the present case, and are independent of D_O.

Our calculations show also that there is only a very weak variation of either u_{FK} or u_∞ when the concentration of oxygen is close to that of air at ambient conditions or if there is an oxygen-enriched atmosphere. As in the dependence on D_O shown in Figure 6, u_{FK} slightly exceeds u_∞ under these particular conditions. However, if the concentration of oxygen is reduced, both u_{FK} and u_∞ increase nonlinearly to $u = \infty$ at $Z_O = 0$. There is also a crossing point of u_{FK} and u_∞, but in either case the oxygen concentration has to be reduced to about 1/10 of that at ambient conditions for the critical value of u to be raised by 10%. Thus there would have to be a severe restriction of oxygen in order to extend significantly the safe operating temperature range.

Dependences of u_a^*, u_{FK}, and u_∞ on the heat of reaction

As would be expected, a decrease of the heat of reaction gives rise to an increase of u_a^* (Figure 7). The predicted values of u_a^* become asymptotic to u_∞ at low exothermicity, but follow u_{FK} rather more closely when the chemical reaction has a higher exothermicity. All three parameters u_a^*, u_{FK}, and u_∞ approach ∞ at $q \to 0$.

Discussion

Hitherto, the theoretical interpretation of spontaneous ignition of combustible fluids in hot lagging has been founded solely on classic thermal ignition theory (Gugan, 1974; Britton, 1991), in which the combustion chemistry is represented most simply as a single-step, first-order exothermic reaction. We have shown that this case is one extreme of the critical conditions that may lead to a lagging fire, defined here as the dimensionless critical temperature u_{FK}. However, by further development of thermal ignition theory to encompass the vaporization of the liquid in a tractable way, a criterion (u_∞) is

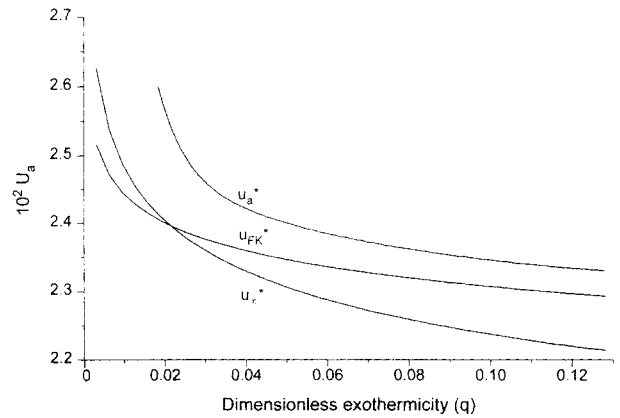

Figure 7. Dependence of u_a^*, u_∞, and u_{FK} on the dimensionless exothermicity of reaction (q); in general, q might vary over the range 0.02 to 0.1.

also derived and tested in the present article to establish when an evaporative control of the hazard occurs. The conditions at which there is a transition from u_{FK} to u_∞ as the most appropriate criterion for safe operation are discussed below.

The primary purpose of the numerical analyses, yielding u_a^*, is to show that u_{FK} or u_∞ represents, with a satisfactory margin of safety, the lowest boundary temperature at which the system would experience thermal runaway. The parameters used in these calculations were derived from an experimental study reported by McIntosh et al. (1994). Any other application of the analytical criteria, expressed either as u_{FK} or u_∞, would require parameters to be derived independently.

While the qualitative departure from u_{FK} to u_∞ as the volatility increases is also well illustrated experimentally in Figure 3, there are aspects of these particular experimental results (McIntosh et al., 1994) that may account for the observed transition to u_∞ being less marked than that which is predicted numerically. These special features are discussed in the next subsection.

Real-time responses

An example of typical, predicted real-time behavior leading up to ignition may be deduced from Figure 2. Ignition is reached after about $3.5 \times t_F$, where t_F is 6,750 s (1.875 h) for a 5-cm cube (Tables 1 and 2). Thus, in this particular case, ignition is predicted to occur about 7 h after the penetration of a flammable liquid into the insulation. As shown in Figure 1, an induction time of this magnitude is approximately a factor of 2 longer than might normally be expected for reactive hydrocarbon fluids adsorbed on a surface. However, it would be between one and two orders of magnitude longer than the time scales that might be attributed to gas-phase oxidation processes (Griffiths and Scott, 1987).

Nevertheless, a predicted induction time of 7 h is considerably shorter than the experimentally measured ignition delays associated with a number of substances investigated by Britton (1991) and also reported elsewhere by us (McIntosh et al., 1994). The substances involved in these abnormal cases tend to be polar in character. We believe that exceptionally strong adsorption forces may be involved in the cohesion to the surface that are strongly influential in the development and eventual occurrence of ignition. Hydrogen bonding of the substrate to the silicate-based insulation is one example of how adhesion can be brought about. The interpretation of behavior of this kind would require a modified structure for the numerical model.

Predictive criteria for criticality and the effect of scale

The main factors that control whether or not there may be a combustion hazard and the ambient temperature at which it may occur are the volatility and loading of the fluid, the exothermicity of the combustion process, and the porosity of the matrix. The oxygen diffusion rate or a reduction in its ambient concentration are influential only close to their limiting conditions. There is also an effect from the shape and size of the insulation, and whether or not there is asymmetric heating. Aspects of scale are confined here to uniform surface heating.

Two simplified dimensionless criteria for ignition, u_∞ and u_{FK}, were introduced in the Theoretical section. These have been compared with the numerical solutions given in the Results section, and in every case they represent lower limiting values of u_a^* for a safe maximum operating temperature. While u_{FK}, which corresponds to the classic Frank-Kamanetskii criterion and also to the Thomas and Bowes (1961) criterion, could be applied in all circumstances, it is most appropriate when there is a low loading of a relatively low volatility fluid and the reaction itself is quite strongly exothermic. In other conditions this criterion leads either to a marked underestimate of a maximum permissible safe working temperature or to the prediction of a potential hazard, even though there may be no hazard in practice. Such application of u_{FK} may impose uneconomic constraints on operating conditions. The predicted watershed temperature is followed more satisfactorily by u_∞ than u_{FK} at high loadings of higher volatility fluids, which may also be an inherently more attractive criterion, because u_∞ incorporates only the properties of the fluid itself.

The conditions that are appropriate for a switch from u_∞ to u_{FK} are given by the crossing point of the curves in Figures 3–5 and 7, and are represented by a transcendental relationship between the principal quantities, as follows:

$$\left[\frac{(1-\beta)}{\left(\ln\dfrac{(q^*a_1^*z^*)}{q_v^*f^*}\right)}\right]^2 \cdot \frac{1}{(q_v^*f^*)^{1/(1-\beta)}} \cdot \frac{1}{x}(q^*a_1^*z^*)^{\beta/(1-\beta)} = \frac{1}{\delta_{cr}}, \quad (15)$$

where * signifies the values taken at the crossing point. Expressing the appropriate terms in dimensional form, Eq. 15 becomes

$$\left[\frac{(1-\beta)}{\left(\ln\dfrac{(Q^*A^*Z^*)}{Q_V^*F^*}\right)}\right]^2 \cdot \frac{1}{(Q_V^*F^*)^{1/(1-\beta)}} \cdot \left(\frac{\lambda E}{p^2 R_{X_O}}\right)(Q^*A^*Z^*)^{\beta/(1-\beta)} = \frac{1}{\delta_{cr}}. \quad (16)$$

However, depending on what we know or wish to know, and also having regard to different physical situations, Eq. 15 or Eq. 16 may be modified to make a specific parameter the subject of the formula. For example, the transition from u_{FK} to u_∞ as the most appropriate criterion when the initial loading (X_O) is increased is given by the equation

$$X_0 = \left[\frac{(1-\beta)}{\ln\left(\dfrac{Q^*A^*Z^*}{Q_V^*F^*}\right)}\right]^2 \cdot \frac{(Q^*A^*Z^*)^{\beta/(1-\beta)}}{(Q_V^*F^*)^{1/(1-\beta)}} \cdot \frac{\delta_{cr}\lambda E}{l^2 R}. \quad (17)$$

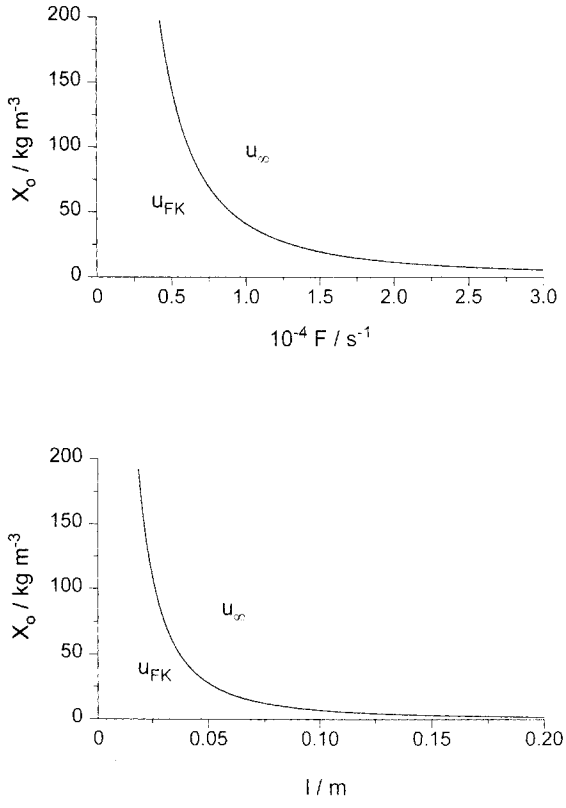

Figure 8. Phase diagrams for liquid fuel density loading (X_O) vs. the characteristic dimension of the insulation (l) or the vaporization rate coefficient (F), respectively.

The region of parameter space in which u_∞ or u_{FK} becomes the most appropriate criticality criterion is marked on each diagram.

A phase plane that represents the dependence of loading on insulation thickness shows that u_∞ becomes the most appropriate criterion at diminishing loadings as the thickness is increased (Figure 8, lower) and a similar observation may be made from the X_O vs. F phase plane (Figure 8, upper). The latter implies that the u_∞ criterion may be more suitable for insulation materials that have an exceedingly high internal surface over which a liquid is dispersed, since the preexponential term for the evaporation rate can be considered a surface-area-dependent parameter.

As interpreted in Figure 8, the effect of scale on the location of the crossing point is governed by the terms encapsulated in δ_{cr} (Eq. 12), which includes a dependence on l^2. It follows that the critical ambient temperature (u_{FK}) normally decreases as the size of the system is increased. Hence, in a large system, the crossing point to favor the u_∞ criterion also moves (1) to a lower value of f (Figure 3), (2) to a higher value of q_v (Figure 4), (3) to a lower loading of fluid (Figure 5), and (4) to a lower ambient concentration of oxygen.

Acknowledgment

The authors gratefully acknowledge financial support of this project from EPSRC (GR/J27431).

Notation

a_1 = reduced preexponential factor for fuel-consumption rate ($= AZ_O t_F$)
a_2 = reduced preexponential factor for oxygen-consumption rate ($= \nu a_1$)
Bi = Biot number
f = reduced preexponential factor for fuel-vaporization rate ($= Ft_F$)
L_O = Lewis number for oxygen within the matrix ($= D_O \rho c/\lambda$)
L_V = Lewis number for fuel vapor within the matrix ($= D_V \rho c/\lambda$)
R = gas constant ($= 8.314\ \mathrm{J \cdot mol^{-1} \cdot K^{-1}}$)
r = linear distance within matrix, m
T_a = ambient temperature, K
$T1/T2$ = Chromel/Alumel thermocouple wires
u_a = dimensionless ambient temperature ($= RT_a/E$)
u_a^* = dimensionless critical temperature obtained numerically
u_∞ = dimensionless temperature at which the rates of exothermic reaction and endothermic vaporization are equal (Eq. 11)
Y_O = initial gaseous density of reactant within the insulation matrix, $\mathrm{kg \cdot m^{-3}}$
y = dimensionless gaseous density of reactant within the insulation matrix
Z_a = external density of oxygen, $\mathrm{kg \cdot m^{-3}}$
β = ratio of activation energies for the heat release and vaporization rates ($= E_v/E$)
τ = dimensionless time ($= t/t_F$)
ξ = dimensionless distance ($= r/l$)

Literature Cited

Aris, R., *The Mathematical Theory of Diffusion and Reaction in Permeable Catalysts*, Clarendon Press, Oxford (1975).
Boddington, T., P. Gray, and D. I. Harvey, "Thermal Theory of Spontaneous Ignition: Criticality in Bodies of Arbitrary Shape," *Phil. Trans. R. Soc. Lond.*, **A270**, 467 (1971).
Bowes, P. C., and B. Langford, "Spontaneous Ignition of Oil-Soaked Lagging," *Chem. Process Eng.*, **49**, 108 (1968).
Bowes, P. C., and P. H. Thomas, "Ignition and Extinction Phenomena Accompanying Oxygen-Dependent Self-Heating of Porous Bodies," *Combust. Flame*, **10**, 221 (1966).
Bowes, P. C., and S. E. Townshend, "Ignition of Combustible Dusts on Hot Surfaces," *Brit. J. Appl. Phys.*, **13**, 105 (1962).
Bowes, P. C., *Self-Heating: Evaluating and Controlling the Hazard*, Her Majesty's Stationery Office, London (1984).
Britton, L. G., "Spontaneous Insulation Fires," *Plant/Oper. Prog.*, **10**, 27 (1991).
Frank-Kamenetskii, D. A., *Diffusion and Heat Transfer in Chemical Kinetics*, (transl. by J. P. Appleton), 2nd ed., Plenum Press, New York (1969).
Gray, B. F., and G. C. Wake, "On the Determination of Critical Ambient Temperatures and Critical Ignition Temperatures for Thermal Ignition," *Combust. Flame*, **71**, 101 (1988).
Gray, B. F., J. H. Merkin, and J. F. Griffiths, "The Prediction of a Practical Lower Bound for Ignition Delay Times and a Method of Scaling Times-to-Ignition in Large Reactant Masses from Laboratory Data," *Symp. on Combustion*, The Combustion Institute, Pittsburgh, p. 1775 (1990).
Gray, P., and P. R. Lee, "Thermal Ignition Theory," *Oxidation and Combustion Reviews*, Vol. 2, C. F. H. Tipper, ed., Elsevier, Amsterdam, p. 1 (1968).
Griffiths, J. F., and S. K. Scott, "Thermokinetic Interactions: Fundamentals of Spontaneous Ignition and Cool Flames," *Prog. Energy Combust. Sci.*, **13**, 161 (1987).
Griffiths, J. F., "Reduced Kinetic Models and Their Application to Practical Combustion Systems," *Prog. Energy Combust. Sci.*, **21**, 25 (1995).
Griffiths, J. F., *Flame and Combustion*, 3rd ed., Chapman & Hall, London (1996).
Gugan, K., "Lagging Fires: The Present Position," *Inst. Chem. Eng. Symp. Ser.*, **39**, 28 (1974).
Lindner, H., and H. Seibring, "Spontaneous Combustion of Organic

Substances in Insulation Materials," *Chem.-Ing.-Tech.*, **39**, 667 (1967).
McIntosh, A. C., M. Bains, W. Crocombe, and J. F. Griffiths, "Autoignition of Combustible Fluids in Porous Insulation Material," *Combust. Flame*, **99**, 541 (1994).
McIntosh, A. C., J. E. Truscott, J. Brindley, J. F. Griffiths, and N. Hafiz, "Spatial Effects in the Thermal Runaway of Combustible Fluids in Insulation Materials," *J. Chem. Soc. Faraday Trans.*, **92**, 2965 (1996).
McIntosh, A. C., B. F. Gray, and G. C. Wake, "Analysis of the Bifurcation Behaviour of a Simple Model of Vapour Ignition in Porous Materials," *Proc. R. Soc. Lond.*, **A453**, 281 (1997).
Mellin, B. E., "Explosion at the BASF Antwerp Ethylene Oxide/Glycol Plant," *Inst. Chem. Eng. Loss Prevention Bulletin*, **100**, 1 (1991).
Snee, T. J., and J. F. Griffiths, "Criteria for Spontaneous Ignition in Exothermic, Autocatalytic Reactions; Chain Branching and Self-Heating in the Oxidation of Cyclohexane in Closed Vessels," *Combust. Flame*, **75**, 381 (1989).
Taradoire, F., "Rapid Oxidation of Drying Oils and 'Anti Oxygens,'" *Comp. R.*, **182**, 61 (1926).
Thomas, P. H., and P. H. Bowes, "Thermal Ignition in a Slab with One Face at a Constant High Temperature," *Trans. Farad. Soc.*, **57**, 2007 (1961).

Manuscript received July 1, 1997, and revision received Feb. 9, 1998.